

# PHOTODETECTION, SELF AMPLIFICATION AND DEMUX OPERATION IN TANDEM AMORPHOUS SI-C DEVICES

*M. Vieira<sup>1,2,3</sup>, P. Louro<sup>1,2</sup>, M. A. Vieira<sup>1,2</sup>, A. Fantoni<sup>1,2</sup>, M. Fernandes<sup>1,2</sup>*

<sup>1</sup> Electronics Telecommunications and Computer Dept, ISEL, Lisbon, Portugal

<sup>2</sup> CTS-UNINOVA, Lisbon, Portugal

<sup>3</sup> DEE-FCT-UNL, Quinta da Torre, Monte da Caparica, 2829-516, Caparica, Portugal

**Keywords:** Optical devices, a-SiC heterostructures, optical communication, multiplexing and demultiplexing applications over POF.

**Abstract:** In this paper we report the use of a monolithic system that combines the demultiplexing operation with the simultaneous photodetection and self amplification of the signal. The device is a double pi'n/pin a-SiC:H heterostructure with optical gate connections for light triggering in different spectral regions. Results show that when a polychromatic combination of different pulsed channels impinges on the device the output signal has a strong nonlinear dependence on the light absorption profile, (wavelength, bit rate and intensity). This effect is due to the self biasing of the junctions under unbalanced light generation of carriers. Self optical bias amplification under uniform irradiation and transient conditions is achieved. An optoelectronic model based on four essential elements: a voltage supply, a monolithic double pin photodiode, optical connections for light triggering, and optical power sources for light bias explains the operation of the optical system.

## 1 INTRODUCTION

There has been much research on semiconductor optical amplifiers as elements for optical signal processing, wavelength conversion, clock recovery, signal demultiplexing and pattern recognition [1]. Here, a specific band or frequency need to be filtered from a wider range of mixed signals. Active filter circuits can be designed to accomplish this task by combining the properties of high-pass and low-pass into a band-pass filter. Amorphous silicon carbon tandem structures, through an adequate engineering design of the multiple layers' thickness, absorption coefficient and dark conductivities [2] can accomplish this function.

Wavelength division multiplexing (WDM) devices are used when different optical signals are encoded in the same optical transmission path, in order to enhance the transmission capacity and the application flexibility of optical communication and sensor systems. Various types of available wavelength-division multiplexers and demultiplexers include prisms, interference filters, and diffraction gratings. Currently modern optical networks use Arrayed Waveguide Grating (AWG) as optical wavelength (de)multiplexers [3] based on multiple waveguides to carry the optical signals

This paper reports results on the use of a double pi'n/pin a-SiC:H WDM heterostructure as an active band-pass filter transfer function whose operation depends on the wavelength of the trigger light and applied voltage and optical bias. The dynamic response can range from positive feedback (regeneration) under positive bias, to two different behaviours under negative bias: as an active multiple-feedback filter with internal gain or in a mode that preserves the amplitude of the signal, depending on the triggering light. An optoelectronic model gives insight on the physics of the system.

## 2 EXPERIMENTAL DETAILS

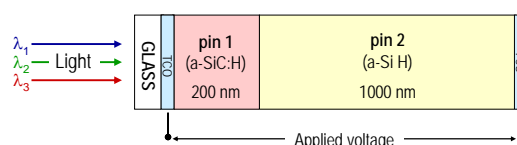


**Figure 1.** Device configuration.

The sensor element is a multilayered heterostructure based on a-Si:H and a-SiC:H produced by PE-CVD at

13.56 MHz radio frequency. The configuration of the device, shown in Figure 1, includes two stacked p-i-n structures (p(a-SiC:H)-i'(a-SiC:H)-n(a-SiC:H)-p(a-SiC:H)-i(a-Si:H)-n(a-Si:H)) sandwiched between two transparent contacts. The thicknesses and optical gap of the front i' (200nm; 2.1 eV) and thick i- (1000nm; 1.8eV) layers are optimized for light absorption in the blue and red ranges, respectively [4]. Experimental details on the preparations, characterizations and optoelectronic properties of the amorphous silicon carbide films and junctions were described elsewhere [5]. As a result, both front and back structures act as optical filters confining, respectively, the blue and the red optical carriers. The device operates within the visible range using as optical signals the modulated light (external regulation of frequency and intensity) supplied by a red (R: 626 nm;  $51\mu\text{W}/\text{cm}^2$ ) a green (G: 524 nm;  $73\mu\text{W}/\text{cm}^2$ ) and a blue (B: 470nm;  $115\mu\text{W}/\text{cm}^2$ ) LED. Additionally, steady state red, green and blue illumination (background) was superimposed using similar LEDs.

### 3 LIGHT FILTERING

The characterization of the devices was performed through the analysis of the photocurrent dependence on the applied voltage and spectral response under different optical and electrical bias conditions. The responsivity was obtained by normalizing the photocurrent to the incident flux. To suppress the *dc* components all the measurements were performed using the lock-in technique.

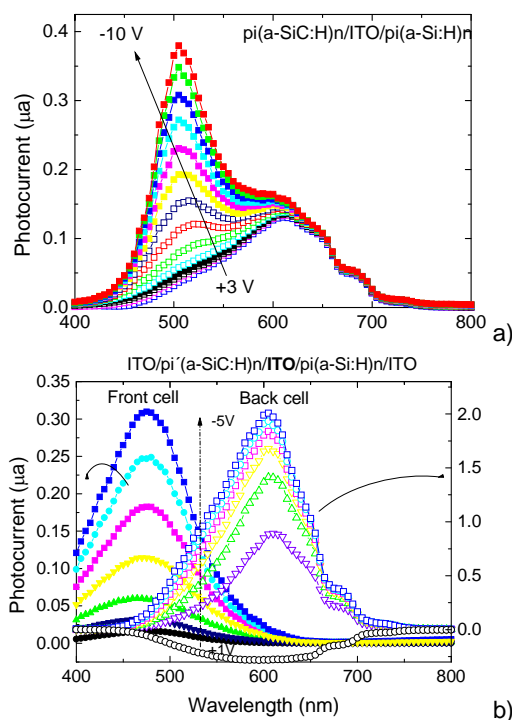


**Figure 2.** a) p-i'-n-p-i-n spectral photocurrent under different applied voltages b) Front, p-i' (a-SiC:H)-n, and back, p-i (a-Si:H)-n spectral photocurrents under different applied bias.

Figure 2a displays the spectral photocurrent of the sensor under different applied bias ( $+3\text{V} < V < -10\text{V}$ ), the internal transparent contact was kept floating in all measurements. In Figure 2b the spectral photocurrent, under different electrical bias is displayed for the front, p-i' (a-SiC:H)-n, and the back p-i (a-Si:H)-n, photodiodes.

Results confirm that the front and back photodiodes act, separately, as optical filters. The front diode, based on a-SiC:H heterostructure, cuts the wavelengths higher than 550nm while the back one, based on a-Si:H, cuts the ones lower than 500nm. Each diode, separately, presents the typical responses of single p-i-n cells with intrinsic layers based on a-SiC:H or a-Si:H materials, respectively. Since the current across the device has to remain the same, in the stacked configuration, it is clearly observed the influence of both front and back diodes modulated by its serial connection through the internal n-p junction.

## 4 SELF OPTICAL AMPLIFICATION

### 4.1 Self bias amplification under uniform irradiation

When an external electrical bias (positive or negative) is applied to a double pin structure, its main influence is in the field distribution within the less photo excited sub-cell [6]. The front cell, under red irradiation; the back cell, under blue light and both, under green steady state illumination. In comparison with thermodynamic equilibrium conditions (dark), the electric field under illumination is lowered in the most absorbing cell (self forward bias effect) while the less absorbing reacts by assuming a reverse bias configuration (self reverse bias effect).

In Figure 3, the spectral photocurrent at different applied voltages is displayed under red (a), green (b) and blue (c) background irradiations and without it (d). Results confirm that a self biasing effect occurs under unbalanced photogeneration. As the applied voltages changes from positive to negative the blue background enhances the spectral sensitivity in the long wavelength range. The red bias has an opposite behavior since the spectral sensitivity is only increased in the short wavelength range. Under green background the spectral photocurrent increases with the applied voltage everywhere.

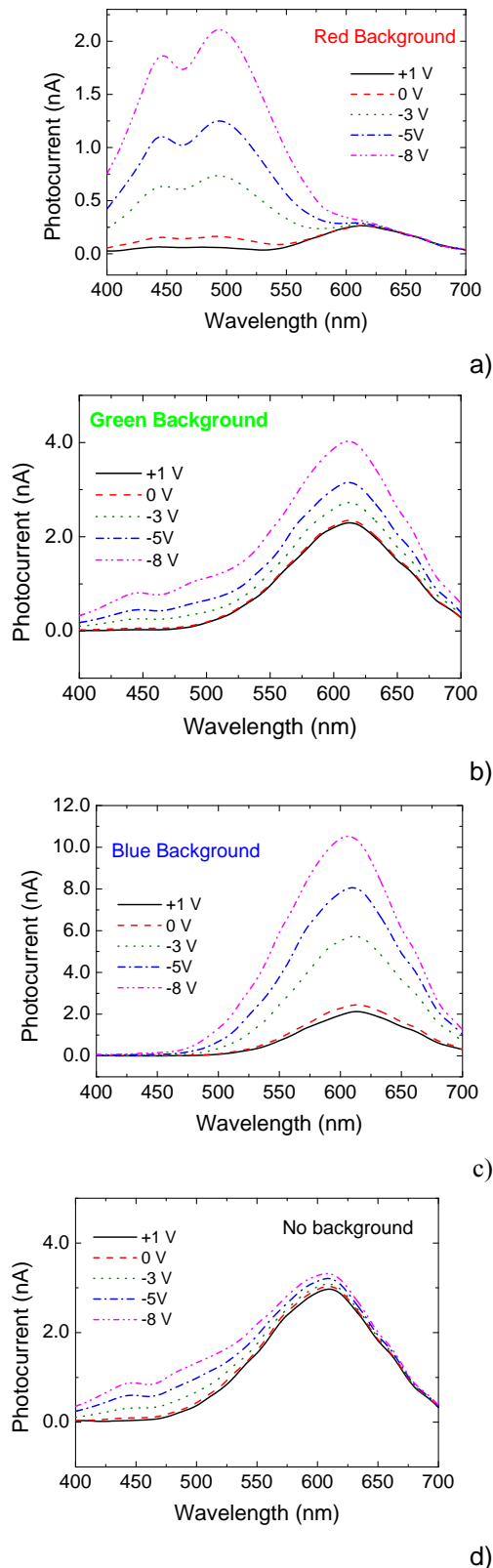


**Figure 3.** Spectral photocurrent under reverse and forward bias measured without and with ( $\lambda_L$ ) background illumination.

In Figure 4 the ratio between the spectral photocurrents @ +1V and -8 V, under red, green and blue steady state illumination and without it (dark), are plotted.

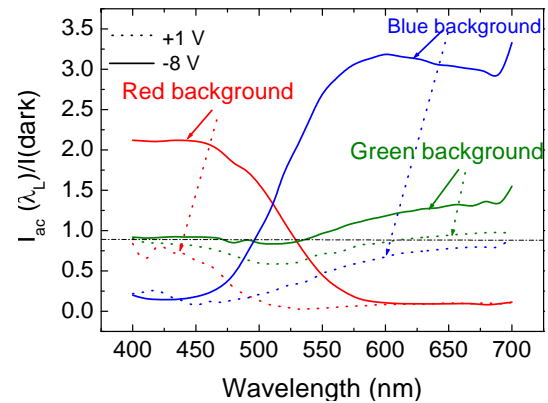


**Figure 4.** Ratio between the photocurrents under red, green and blue steady state illumination and without it (no background).

As expected, results show that the blue background enhances the light-to-dark sensitivity in the long wavelength range and quenches it in the short wavelength range. The red bias has an opposite behavior; it reduces the ratio in the red/green wavelength range and amplifies it in the blue one. The sensor is a wavelength current-controlled device, that make use of changes in the wavelength of the optical bias to control the power delivered to a load, acting as an optical amplifier. Its gain, defined as the ratio between the photocurrent with and without a specific background depends on the background wavelength that controls the electrical field profile across the device. If the electrical field increases locally (self optical amplification) the collection is enhanced and the gain is higher than one. If the field is reduced (self optical quench) the collection is reduced and the gain is lower than one. This optical nonlinearity makes the transducer attractive for optical communications.

#### 4.2 Self bias amplification under transient conditions and uniform irradiation

A chromatic time dependent wavelength combination (4000 bps) of R ( $\lambda_R=624$  nm), G ( $\lambda_G=526$  nm) and B ( $\lambda_B=470$  nm) pulsed input channels with different bit sequences, was used to generate a multiplexed signal in the device. The output photocurrents, under positive (dot arrows) and negative (solid arrows) voltages with (colour lines) and without (dark lines) background are displayed in Figure 5. The bit sequences are shown at the top of the figure.

Results show that, even under transient input signals (the input channels), the background wavelength controls the output signal as in Figures 3 and 4. This nonlinearity, due to the transient asymmetrical light penetration of the input channels across the device together with the modification on the electrical field profile due to the optical bias, allows tuning an input channel without demultiplexing the stream.

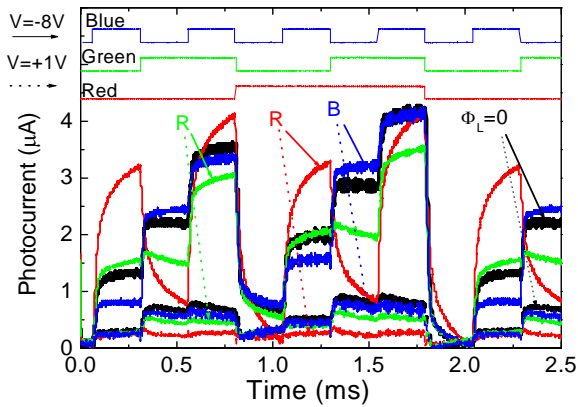


**Figure 5.** Single and combined signals @-8V; without (solid arrows) and with (dotted arrows) green optical bias.

In Figure 6 the green channel is tuned through the difference between the multiplexed signal with and without green bias.

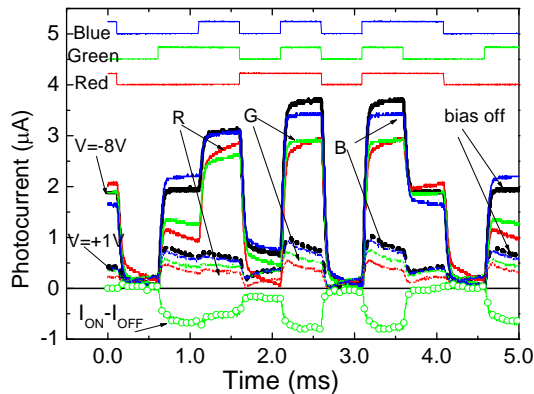


**Figure 6.** Multiplexed signals @-8V/+1V (solid /dot lines); without (bias off) and with (R, G, B) green optical bias.

## 5 WAVELENGTH-DIVISION (DE)MULTIPLEXING DEVICE

In this section we report the use of the same devices to combines the demultiplexing operation with the simultaneous photodetection of the signal.

The device makes use of the fact that the optical absorption of the different wavelengths can be tuned by means of electrical bias changes or optical bias variations (Figure 5 and Figure 6). This capability was obtained using adequate engineering design of the multiple layers thickness, absorption coefficient and dark conductivities [7]. The device described herein operates from 400 to 700 nm which makes it suitable for operation at visible wavelengths in optical communication applications.

Monochromatic pulsed beams together or one single polychromatic beam (mixture of different wavelength) impinge in the device and are absorbed, according to their wavelength (Figure 7). By reading out, under appropriate electrical bias conditions, the photocurrent

generated by the incoming photons, the input information is electrically multiplexed or demultiplexed.

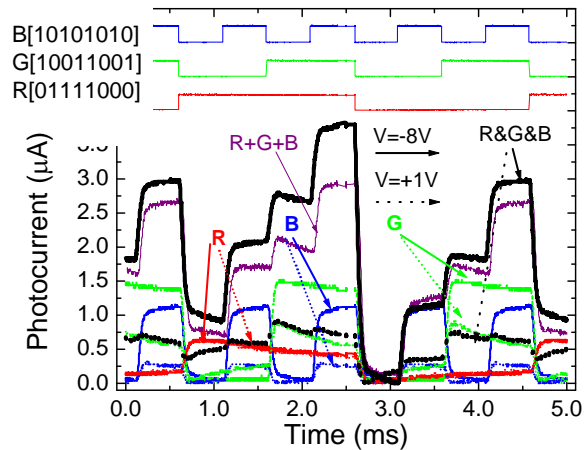


**Figure 7.** Single (R, G and B) and combined (R&G&B) signals under -8V (solid arrows) and +1V (dotted arrows).

In the multiplexing mode the device faces the modulated light incoming together (monochromatic input channels). The combined effect of the input signals is converted to an electrical signal, via the device, keeping the input information (wavelength, intensity and modulation frequency). The output multiplexed signal, obtained from the combination of the three optical sources, depends on both the applied voltage and on the ON-OFF state of each input optical channel. Under negative bias, the multiplexed signal presents eight separate levels. The highest level appears when all the channels are ON and the lowest if they are OFF. Furthermore, the levels ascribed to the mixture of three or two input channels are higher than the ones due to the presence of only one (R, G, B). Optical nonlinearity was detected; the sum of the input channels (R+B+G) is lower than the correspondent multiplexed signals (R&G&B). This optical amplification, mainly on the ON-ON states, suggests capacitive charging currents due to the time-varying nature of the incident lights. Under positive bias the levels were reduced to one half since the blue component of the combined spectra falls into the dark level, the red remains constant and the green component decreases.

In the demultiplexing mode a polychromatic modulated light beam is projected onto the device and the readout performed by shifting between forward and reverse bias.

Figure 7 displays the input and multiplexed signals under negative (-8V) and positive (+1V) electrical bias. As expected, the input red signal remains constant while the blue and the green ones decrease as the voltage changes from negative to positive.

To recover the transmitted information (8 bit per wavelength channel) the multiplexed signal, during a complete cycle, was divided into eight time slots, each corresponding to one bit where the independent optical signals can be ON (1) or OFF (0). Under positive bias, the device has no sensitivity to the blue channel, so the red



and green transmitted information are tuned and identified. The highest level corresponds to both channels ON ( $R=1, G=1$ ), and the lowest to the OFF-OFF stage ( $R=0, G=0$ ). The two levels in-between are related with the presence of only one channel ON, the red ( $R=1, G=0$ ) or the green ( $R=0, G=1$ ). To distinguish between these two situations and to decode the blue channel, the correspondent sub-levels, under reverse bias, have to be analyzed. The highest increase at  $-8V$  corresponds to the blue channel ON ( $B=1$ ), the lowest to the ON stage of the red channel ( $R=1$ ) and the intermediate one to the ON stage of the green ( $G=1$ ). Using this simple key algorithm the independent red, green and blue bit sequences were decoded as:  $R [01111000]$ ,  $G[10011001]$  and  $B[10101010]$  which are in agreement with the signals acquired for the independent channels.

## 6 THE OPTOELECTRONIC MODEL.

### 6.1 Two connected transistor model

Based on the experimental results and device configuration an optoelectronic model was developed [8] which is displayed in Figure 8. The optoelectronic block diagram (a) consists of four essential elements: a double pin device for detection, a voltage supply to  $dc$  voltage bias; optical connections for light triggering and optical bias to  $dc$  light bias control. These four elements when connected together form the essentials of the optoelectronic circuit.

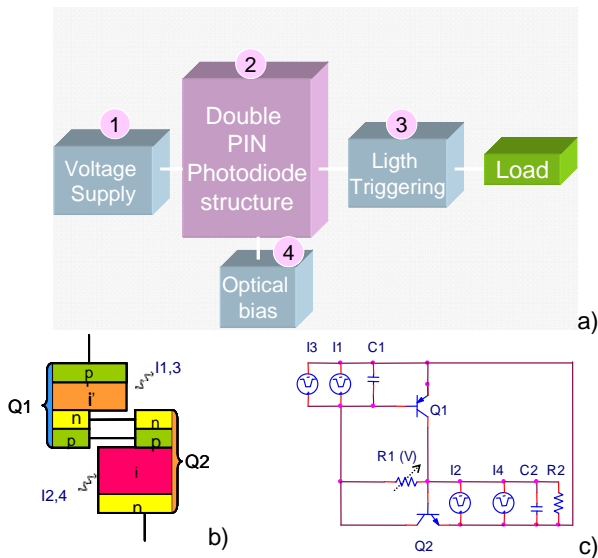


**Figure 8.** a) Optoelectronic block diagram. b) Compound connected phototransistor equivalent model. c) ac equivalent circuit.

The monolith device is modelled by the two-transistor model ( $Q_1$ - $Q_2$ ) (Figure 8b) that can be considered to constitute *pnp* ( $Q_1$ ) and *nnp* ( $Q_2$ )

phototransistors separately. The *ac* circuit representation is displayed in Figure 8c.

Its operation is based upon the following principle: the flow of current through the resistor connecting the two transistor bases is proportional to the difference in the voltages across both capacitors (charge storage buckets). Two optical gate connections ascribed to the different light penetration depths across the front ( $Q_1$ ) and back ( $Q_2$ ) phototransistors were considered to allow independent blue ( $I_1$ ), red ( $I_2$ ) and green ( $I_3, I_4$ ) channels transmission. Four square-wave current sources with different intensities are used; two of them,  $I_1$  and  $I_2$ , with different frequencies to simulate the input blue and red channels and other two,  $I_3$  and  $I_4$ , with the same frequency but different intensities to simulate the green channel due to its asymmetrical absorption across both front and back phototransistors. The charge stored in the space-charge layers is modelled by the capacitor  $C_1$  and  $C_2$ .  $R_1$  and  $R_2$  model the dynamical resistances of the internal and back junctions under different *dc* bias conditions.

Once the *ac* sources are connected in the load loop an *ac* current flows through, establishing voltage modifications across the two capacitors. During the simultaneous transmission of the three independent bit sequences, the set-up in this capacitive circuit loop is constantly changing in magnitude and direction. This means that the voltage across one capacitor builds up until a maximum and the voltage across the other builds up to a minimum. The system collapses and builds up in the opposite direction. It tends to saturate and then leave the saturation because of the cyclic operation. This results in changes on the reactance of both capacitors. The use of separate capacitances on a single resistance  $R_1$  results in a charging current gain proportional to the ratio between collector currents. The *dc* voltage, according to its strength, aids or opposes the *ac* currents.

### 6.2 Optoelectronic simulation

The multiplexed signal was simulated by applying the Kirchhoff's laws for the simplified *ac* equivalent circuit (Figure 8c) and the four order Runge-Kutta method to solve the corresponding state equations.

$$\frac{dv_{1,2}}{dt} = \begin{bmatrix} -\frac{1}{R_1 C_1} & \frac{1}{R_1 C_1} \\ \frac{1}{R_1 C_2} & -\frac{1}{R_1 C_2} - \frac{1}{R_2 C_2} \end{bmatrix} v_{1,2}(t) + \begin{bmatrix} \frac{1}{C_1} \\ \frac{1}{C_2} \end{bmatrix} i_{1,2}(t) \quad (1)$$

$$i(t) = \begin{bmatrix} 0 & \frac{1}{R_2} \end{bmatrix} v_{1,2}(t) \quad (2)$$

with  $v_1(t)$  and  $v_2(t)$  the emitter-base voltages of  $Q_1$  and  $Q_2$  transistors and  $i(t)$  the generated photocurrent under transient conditions. MATLAB was used as a programming environment and the input parameters

chosen in compliance with the experimental results (Figure 7).

In Figure 9 the simulated currents (symbols) under negative and positive bias are compared. In Figure 10 and under negative bias the simulated current under green (a) and red backgrounds are displayed. The current sources are also displayed (dash lines). To simulate the red and the green backgrounds, current sources intensities were multiplied by the on/off ratio between the input channels with and without optical bias. The same bit sequence of Figure 7 was used. To validate the model the experimental multiplexed signals are also shown (solid lines).

Good agreement between experimental and simulated data was observed. Under negative bias and if no optical bias is applied, the expected eight levels are detected, each one corresponding to the presence of three, two, one or no color channel ON. Under positive bias or steady state irradiation the levels are amplified or reduced depending on the external control. The expected optical amplification is observed due to the effect of the active multiple-feedback filter when the back diode is light triggered.

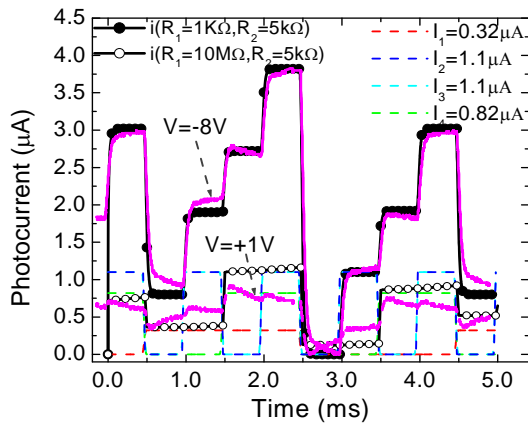


**Figure 9.** Multiplexed simulated (symbols), current sources (dash lines) and experimental (solid lines) under negative ( $R_1=1K\Omega$ ;  $-8V$ ) and positive ( $R_1=10M\Omega$ ;  $+1V$ ) dc bias without any background.

Under forward bias (high  $R_1$ ) the device remains in its non conducting state unless a light pulse ( $I_2$  or  $I_2+I_4$ ) is applied to the base of  $Q_2$ . This pulse causes  $Q_2$  to conduct because the reversed biased n-p internal junction behaves like a capacitor inducing a charging current ( $I_2+I_4$ ) across both collector junctions. The collector of the conducting transistor pulls low, moving the  $Q_1$  base toward its collector voltage, which causes  $Q_1$  to conduct. The collector of the conducting  $Q_1$  pulls high, moving the  $Q_2$  base in the direction of its collector. This positive feedback (regeneration) reinforces the  $Q_2$  already conducting state and a current  $I_2+I_4$  will flow on the external circuit.

Green irradiation (Figure 10a) moves asymmetrically the  $Q_1$  and  $Q_2$  bases toward their emitter voltages, resulting in lower values of  $I_3$  and  $I_4$  when compared without optical bias.  $I_1$  and  $I_2$  slightly increase due to the

increased carrier generation on the less absorbing phototransistors. Under negative bias During the duration of the red and blue pulses ( $I_1$  or  $I_2$  ON), as without optical bias, the internal junction remains forward biased and the transferred charge between  $C_1$  and  $C_2$  reaches the output terminal as a capacitive charging current. During the green pulse ( $I_3$  and  $I_4$  ON) only residual charges are transferred between  $C_1$  and  $C_2$ . So, only the charges generated in the base of  $Q_2$  ( $I_4$ ) reaches the output terminal as can be confirmed by the good fitting between simulate and experimental differences of both multiplexed signals without and with optical bias. Under red background the expected optical amplification in the low wavelength range is observed (Figures 3a and 4) due to the effect of the active multiple-feedback filter when the back diode is light triggered

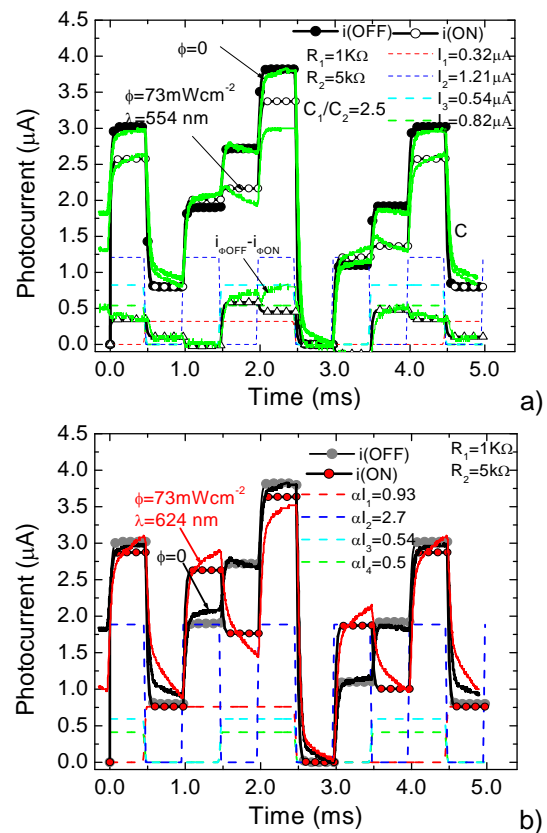


**Figure 10.** Multiplexed simulated (symbols), current sources (dash lines) and experimental (solid lines): under negative ( $R_1=10M\Omega$ ;  $-8V$ ) and positive ( $R_1=1k\Omega$ ;  $+1V$ ) dc bias and green (a) and red (b) backgrounds.

### 6.3 Transfer characteristics

To illustrate the transfer characteristics effects due to changes in steady state light, dc control voltage or applied light pulses the following steps in the operation and control of the optoelectronic circuit are considered:

1 *Positive voltage bias control.* Only an ac current is flowing through the load capacitance  $C_2$ . The device has high ohmic resistance (high  $R_1$ ) and remains in its

non conducting state unless a light pulse ( $I_2$  or  $I_2+I_4$ ) is applied to the base of  $Q_2$ . This pulse causes  $Q_2$  to conduct as the reversed biased n-p internal junction behaves like a capacitor inducing a charging current across  $R_2$ . No amplification effect was detected since  $Q_1$  acts as a load and no charges are transferred between  $C_1$  and  $C_2$  (Figure 6a).

2 *Negative dc voltage bias control.* Under negative bias the device has low ohmic resistance (low  $R_1$ ) the base emitter junction of both transistors are inversely polarized and conceived as phototransistors, thus taking advantage of the amplifier action of neighboring collector junctions, which are polarized directly. This results in a charging current gain proportional to the ratio between both collector currents ( $C_1/C_2$ ). The device behaves like an optoelectronic controlled transmission system that stores, amplifies and transports the minority carriers generated by the current pulses, through the capacitors  $C_1$  and  $C_2$ . Here, the *dc* voltage control creates a voltage across one or both capacitors which, when superimposed with an *ac* pulse, collectively saturates the circuit. No additional change in the voltage across the capacitors occurs. This results in maximum power transfer to the load.

3 *Optical bias control.* Depending on it wavelength (Figures 3 and Figure 4) the optical bias changes the amplitude of the *ac* current sources by an  $\alpha$  factor, and so the voltages across one or both capacitors. Blue, red or green irradiations move asymmetrically the bases of  $Q_1$ ,  $Q_2$  or both toward their emitter voltages (self-forward effect), resulting, respectively in lower values of  $I_1$ ,  $I_2$ ,  $I_3$  and  $I_4$  when compared with no optical bias. The circuit can leave the saturation resulting in a wavelength controlled power transfer to the load that allows tuning input channel from the stream (Figure 10).

Results also show that the two-transistor model explains the difference between the conduction mechanisms, under positive and negative bias, helping to understand the signal decoding algorithm. Under positive bias the red and green channels are immediately decoded since the collected current is due exclusively to the generated carriers at the back diode. Under negative bias, depending on the ratio between  $C_1$  and  $C_2$ , different charging currents across the reversed junctions have to be considered. The balance between them depends on the presence of three, two or one channel ON (Fig. 2-3). So, by comparing the different sublevels signals under positive and negative bias it is possible to recover the blue, the green and the red input channels.

## 7 CONCLUSIONS

A double  $\pi$ -n/pin a-SiC:H heterostructure with optical gate connections was presented. Multiple monochromatic pulsed communication channels were transmitted together and the multiplexed signal analyzed at different electrical and optical bias. Results show that the output signal has a strong nonlinear dependence on the light absorption profile. This effect is due to the self biasing of the junctions under unbalanced light generation profiles. Self optical bias amplification under uniform irradiation and transient conditions is achieved. An optoelectronic model based on four essential elements: a voltage supply; a double pin photodiode; optical connections for light triggering and optical power sources for light bias explains the operation of the optical system.

## REFERENCES

- [1] M. J. Connelly, Semiconductor Optical Amplifiers. Boston, MA: Springer-Verlag, 2002. ISBN 978-0-7923-7657-6.
- [2] P. Louro, M. Vieira, Yu. Vygranenko, A. Fantoni, M. Fernandes, G. Lavareda, N. Carvalho Mat. Res. Soc. Symp. Proc., 989, A12.04 (2007).
- [3] Michael Bas, Fiber Optics Handbook, Fiber, Devices and Systems for Optical Communication, Chap, 13, Mc Graw-Hill, Inc. 2002.
- [4] M. Vieira, A. Fantoni, M. Fernandes, P. Louro, G. Lavareda, C. N. Carvalho, Journal of Nanoscience and Nanotechnology, Vol. 9 , Number 7, July 2009 , pp. 4022-4027(6).
- [5] M. Vieira, M. Fernandes, P. Louro, A. Fantoni, M. A. Vieira, J. Costa, M. Barata, Mat. Res. Soc. Symp. Proc. Volume 1245, A08-02 (2010) .
- [6] M. Vieira, A. Fantoni, P. Louro, M. Fernandes, R. Schwarz, G. Lavareda, and C. N. Carvalho, Vacuum, Vol. 82, Issue 12, 8 August 2008, pp: 1512-1516.
- [7] P. Louro, M. Vieira, Yu. Vygranenko, A. Fantoni, M. Fernandes, G. Lavareda, N. Carvalho Mat. Res. Soc. Symp. Proc., 989 (2007) A12.04.
- [8] M. A. Vieira, M. Vieira, M. Fernandes, A. Fantoni, P. Louro, M. Barata, Amorphous and Polycrystalline Thin-Film Silicon Science and Technology 2009, MRS Proceedings Vol. 1153, A08-0.